Evaluation of the effectiveness of air pollution control measures in Hong Kong[☆]

X.P. Lyu [a], L.W. Zeng [a], H. Guo [a, *], I.J. Simpson [b], Z.H. Ling [a], Y. Wang [a], F. Murray [c], P.K.K. Louie [d], S.M. Saunders [e], S.H.M. Lam [e, f], D.R. Blake [b]

[a] Department of Civil and Environmental Engineering, The Hong Kong Polytechnic University, Hong Kong
[b] Department of Chemistry, University of California at Irvine, CA, USA
[c] Environmental Science, Murdoch University, Perth, Australia
[d] Environmental Protection Department, Hong Kong
[e] School of Chemistry and Biochemistry, University of Western Australia, Perth, Australia
[f] Pacific Environment Limited, Perth, Australia

ARTICLE INFO

ABSTRACT

From 2005 to 2013, volatile organic compounds (VOCs) and other trace gases were continuously measured at a suburban site in Hong Kong. The measurement data showed that the concentrations of most air pollutants decreased during these years. However, ozone (O_3) and total non-methane hydrocarbon levels increased with the rate of 0.23 ± 0.03 and 0.34 ± 0.02 ppbv/year, respectively, pointing to the increasing severity of photochemical pollution in Hong Kong. The Hong Kong government has ongoing programs to improve air quality in Hong Kong, including a solvent program implemented during 2007—2011, and a diesel commercial vehicle (DCV) program since 2007. From before to after the solvent program, the sum of toluene, ethylbenzene and xylene isomers decreased continuously with an average rate of -99.1 ± 6.9 pptv/year, whereas the sum of ethene and propene increased by 48.2 ± 2.0 pptv/year from before to during the DCV program. Despite this, source apportionment results showed that VOCs emitted from diesel exhaust decreased at a rate of -304.5 ± 17.7 pptv/year, while solvent related VOCs decreased at a rate of -204.7 ± 39.7 pptv/year. The gasoline and liquefied petroleum gas vehicle emissions elevated by 1086 ± 34 pptv/year, and were responsible for the increases of ethene and propene. Overall, the simulated O_3 rate of increase was lowered from 0.39 ± 0.03 to 0.16 ± 0.05 ppbv/year by the solvent and DCV programs, because O_3 produced by solvent usage and diesel exhaust related VOCs decreased ($p < 0.05$) by 0.16 ± 0.01 and 0.05 ± 0.01 ppbv/year between 2005 and 2013, respectively. However, enhanced VOC emissions from gasoline and LPG vehicles accounted for most of the O_3 increment (0.09 ± 0.01 out of 0.16 ± 0.05 ppbv/year) in these years. To maintain a zero O_3 increment in 2020 relative to 2010, the lowest reduction ratio of VOCs/NOx was ~1.5 under the NOx reduction of 20 —30% which was based on the emission reduction plan for Pearl River Delta region in 2020.

© 2016 Elsevier Ltd. All rights reserved.

1. Introduction

As a special administrative region of China, Hong Kong has been one of the most developed regions in Asia since the early 1990s. With the rapid development of the economy in Hong Kong and the adjacent inland Pearl River Delta (PRD) region, air pollution has inevitably emerged, particularly photochemical smog (Ling and Guo, 2014; Xue et al., 2014; Guo et al., 2013). Due to the adverse effects of photochemical pollution on the environment and human health (Thurston and Ito, 1999; Lippmann, 1992), extensive control measures have been taken in many cities around the world (Carvalho et al., 2015; Derwent et al., 2010), including Hong Kong (see http://www.epd.gov.hk/epd/english/environmentinhk/air/air_maincontent.html), where photochemical pollution is severe.

Table S1 in the Supplementary Material summarizes the main control measures implemented in Hong Kong for improving air quality in the past decade, which has placed emphasis on reducing emissions of air pollutants from three sources, i.e., diesel-fueled

vehicles, solvent usage and LPG-fueled vehicles. The emission control measures for diesel commercial vehicles (DCVs), referred to as the DCV program, were initiated in April 2007 and have continued to the present. This stepwise program was designed to eliminate high emission diesel vehicles and promote the upgrade of emission requirements to Euro IV standard (see http://ec.europa.eu/environment/air/transport/road.htm). During the first stage of the DCV program (April 2007–March 2010), ~1700 (30% of all DCVs) pre-Euro and Euro I DCVs were eliminated or upgraded to meet the Euro IV emission standard. With the upgrade of emission standards from pre-Euro and Euro I to Euro IV, it was expected that the VOCs and NO$_x$ emissions would decrease by 2/3 and 1/2, respectively. The second stage of the DCV program (July 2010–June 2013) required ~7400 (27% of all DCVs) comprising Euro II DCVs to be eliminated or upgraded in emission standard to meet Euro IV, which required a VOC and NO$_x$ emission reduction of 50% per vehicle relative to Euro II. In March 2014, an incentive policy was further enforced to ensure that all DCVs in Hong Kong complied with the Euro IV emission standard by the end of 2019, which means that ~82,000 DCVs would be eliminated or upgraded in emission standard. Therefore, the DCV program is considered to be essentially continuous from 2007 to the present. Another important measure on VOC control in Hong Kong was the solvent program, which focused on regulating the maximum contents of VOCs in solvent products, i.e., printing ink, hairspray, architectural paint, air fresheners, paint and coatings used in vehicle refinishing, adhesives and sealants. In addition, it required the installation of emission reduction devices on printing machines. For example, all the lithographic heatset web printing machines were required to have emission reduction devices installed to ensure that VOC levels in the waste gases were lower than 100 mg carbon/m^3. The solvent program was mainly carried out during 2007–2011.

In addition to the DCV and solvent programs, prompt action was taken to lower the VOC emission from LPG fueled vehicles (mainly propane and i-/n-butanes) during September 2013–May 2014, when worn catalytic converters on ~17,000 LPG-fueled vehicles (65% of all LPG-fueled vehicles) were replaced. A study by our group (Lyu et al., 2016) confirmed the effectiveness of this measure on the reduction of NO$_x$ and LPG-related VOCs at a roadside site in Hong Kong. Hence, the effect of the LPG catalytic converter replacement was not discussed in this study, also because this study ends in 2013 before the LPG control measures were fully implemented.

Despite the measures that have been implemented, Hong Kong still suffers from episodes of severe air pollution, particularly photochemical smog. Ground-level O$_3$ levels have increased continuously in Hong Kong in the past decade (Xue et al., 2014; Zhang et al., 2007; HKEPD, 2014), although the concentrations of most primary air pollutants have decreased. Since O$_3$ is a product of the reactions between VOCs and NO$_x$ in the presence of solar radiation, in order to effectively control O$_3$ pollution, changes in the levels of O$_3$ precursors and the effects of the control measures on O$_3$ pollution need to be studied. The outcomes are helpful to formulate future control measures for O$_3$ abatement. It is noteworthy that as Hong Kong is adjacent to the inland PRD, and regional impacts on air quality in Hong Kong have been demonstrated in many studies (e.g., Cheng et al., 2013; Ding et al., 2013; Guo et al., 2009), it is crucial to exclude the regional impact when local control measures are evaluated.

In this study, the long term trends of air quality in Hong Kong from 2005 to 2013 were investigated to provide a comprehensive evaluation of the changes of primary air pollutants and subsequent impact on O$_3$ production resulting from the DCV and solvent programs. Furthermore, the ground-level O$_3$ production in 2020 was estimated under the planned reduction targets of VOCs and NO$_x$, and the optimal reduction ratios of VOCs/NO$_x$ for a zero O$_3$

increment were determined.

2. Methodology

2.1. Site description and data collection

Hong Kong is located on the coast of southern China, neighboring Guangdong province to the north, the Pearl River Estuary to the northwest, and the South China Sea (SCS) to the south and east. It constitutes the greater PRD with Macau and nine mainland cities (Fig. S1 in the Supplementary Material). Northerly and northeasterly winds are dominant in cold seasons, while the southerly winds from the SCS prevail in warm seasons. The monitoring site (Tung Chung, TC) was located in a new residential town of western Hong Kong. The main local pollution sources are traffic at a nearby airport highway, aircraft at the Hong Kong international airport (~3 km to the northwest) and residential activities. In addition, urban emissions in the northeast part of Hong Kong also contributed to this site when the prevailing winds were from northeast direction during most time periods of a year. Furthermore, since it is adjacent to the inland PRD and Macau, TC was also a receptor of air pollution from those regions. Therefore, this site was an ideal location to characterize the local and regional air pollution (Cheng et al., 2010; Guo et al., 2009).

Real-time measurements of twenty-nine VOC species, five other trace gases (SO$_2$, CO, NO, NO$_2$ and O$_3$), and meteorological parameters were continuously conducted by the Hong Kong Environmental Protection Department (HKEPD). Table S2 in the Supplementary Material provides the instruments, analysis techniques, detection limits and time resolutions of the measurements, if available. Details about the measurements and quality control protocols can also be found in Ou et al. (2015), HKEPD (2014) and Ling et al. (2013).

2.2. Filtration of local air masses

To study the trends of local air quality and to evaluate the effects of local control measures, the impact from regional air masses was minimized in our analysis according to hourly wind speeds (WS), as follows. The local air masses were selected using WS lower than 2 m/s, i.e. when the air was generally still or calm (Beaufort Wind Scale, http://www.spc.noaa.gov/faq/tornado/beaufort.html). This method has been used and confirmed to be reasonable in previous studies (Guo et al., 2013; Cheung et al., 2010). Fig. S2 in the Supplementary Material shows the average wind field distribution at TC from 2005 to 2013. The prevailing winds were from the east, where the urban centers of Hong Kong located. Furthermore, the ratios of SO$_2$/NO$_x$ and CO/NO$_x$ at TC were calculated for the scenarios with wind speed $\geq$ and <2 m/s, respectively. It was found that SO$_2$/NO$_x$ and CO/NO$_x$ were 0.12 ± 0.01 and 9.86 ± 0.41 at wind speed <2 m/s, respectively, within the ranges of 0.07–0.12 and 7.71–14.2 for the urban sites in Hong Kong, respectively (Fig. S3 in the Supplementary Material). In contrast, the SO$_2$/NO$_x$ (0.15 ± 0.01) and CO/NO$_x$ (15.54 ± 0.56) at wind speed $\geq$ 2 m/s exceeded their upper limits for the urban sites in Hong Kong. On the other hand, the ratio of benzene/toluene at TC was 0.54 ± 0.02 at wind speed <2 m/s, comparable to the typical value from vehicular exhaust (~0.5) (Scheff and Wadden, 1993), while much lower than that (3.4) in aged air masses (roughly represents regional and superregional transport) identified by Lau et al. (2010). These signatures increased the reasonability of this method. However, the regional transport was not expected to be completely eliminated, which might slightly enhance the increment of the simulated O$_3$. According to the filtration, the local air masses (WS < 2 m/s) accounted for 60.5% of the total air masses arriving at TC, and are used hereafter unless

otherwise specified.

The filtration of local air masses, along with the missing data due to instrument maintenance, led to the data unavailability in some periods. However, the missing data accounted for only 17.6% of all the data of local air masses, and most of the data were available at both the beginning and the end of the study periods which largely determined the slopes and trends. The missing data would not affect the overall slopes and trends significantly, due to the fact 1) source emissions of air pollutants were relatively stable, and 2) meteorological conditions had no significant changes between 2005 and 2013 ($p > 0.1$) in Hong Kong (Fig. S4 in the Supplementary Material). Hence, it is reasonable to speculate that abrupt changes of air pollutant levels do not occur.

2.3. Model construction and application

The positive matrix factorization (PMF) model was used to resolve the sources of VOCs. Since the detailed operation principle of the model has been thoroughly described (Paatero, 1997; Paatero and Tapper, 1994), we only provide the configurations for model input and running. The hourly concentrations of VOCs and trace gases (CO, NO and NO_2) with a proportion of missing values less than 25% were included in the input file. Values lower than the detection limit (DL) were replaced with DL/2. The uncertainties were set as $\sqrt{(10\% \times concentration)^2 + DL^2}$ and $5/6 \times DL$ for the samples with their concentrations higher and lower than the DL, respectively. The model ran 20 times with a random seed, and the optimum solution automatically recommended by the model was accepted. It should be noted that CO, NO and NO_2 were used to help identify but not quantify the sources in this study, because some of their important sources might be missing in this source apportionment. For example, the Hong Kong Emission Inventory indicated that ~31% of NO_x is emitted from public electricity generation (HKEPD, 2013). However, this source could not be identified with the selected VOCs and trace gases as input.

A photochemical box model incorporating the master chemical mechanism (PBM-MCM) was utilized to simulate the local O_3 formation. In addition to the explicit chemical mechanism, photolysis rates, boundary layer height and dry deposition were also considered in the model. The PBM-MCM model has been well applied to Hong Kong data for simulation (Ling et al., 2014; Lam et al., 2013). In this study, the hourly measurements of VOCs, trace gases and meteorological parameters (temperature and relative humidity) at TC were used to construct the model. The daytime (07:00—19:00) simulations were conducted for the whole sampling period except for rainy days. More details about the mechanism, construction and application of the PBM-MCM model are provided in Section S1 "Model description" in the Supplementary Material. Fig. 1 shows

the monthly average diurnal patterns of the simulated and observed O_3 from 2005 to 2013 for all air masses at TC. In general, the simulated O_3 fit the observed values well in terms of magnitude and seasonal/diurnal patterns. To quantitatively evaluate the performance of the model, several statistical parameters were calculated. The index of agreement (IOA) represents better agreements between the simulated and observed O_3 with increasing values in the range of 0—1, and was calculated using equation (1) (Hurley et al., 2001):

$$IOA = 1 - \frac{\sum_{i=1}^{n}(O_i - S_i)^2}{\sum_{1i=1}^{n}\left(|O_i - \overline{O}| + |S_i - \overline{O}|\right)^2} \tag{1}$$

where O_i and S_i are the hourly observed and simulated values, respectively. $\overline{O}$ represents the observed average of the n samples. Although the overall simulated O_3 average during 2005—2013 (26.0 ± 0.3 ppbv) was slightly lower than the observed average (29.7 ± 0.4 ppbv), the positive (33.4 ± 0.8%) and negative bias (−26.1 ± 0.5%) were acceptable. Moreover, IOA reached 0.77, indicating that the model well reproduced the observed O_3.

3. Results and discussion

3.1. Air quality trends

Table 1 summarizes hourly mean values with standard deviations (S.D.), national standard levels and the yearly variation rates of the main air pollutants in the local air masses at TC from 2005 to 2013. Year 2007 was not included due to the lack of data. The hourly average mixing ratios of all the air pollutants were much lower than the national standards, if available. Furthermore, the mixing ratios of SO_2, CO, NO and NO_2 decreased, at an average rate of −0.44 ± 0.01, −17.1 ± 0.4, −0.37 ± 0.04 and −0.13 ± 0.03 ppbv/year, respectively. The results suggest that the air quality in Hong Kong was generally in good shape. However, the hourly maximum NO_2 (951.8 ppbv) and O_3 (184.9 ppbv) far exceeded the corresponding national standards (106 ppbv for both NO_2 and O_3). Furthermore, the total non-methane hydrocarbons (NMHCs) showed an increasing trend throughout the study period, of 0.34 ± 0.02 ppbv/year. The increasing trend of the total NMHCs was opposite to that indicated by the emission inventory in Hong Kong, in which the VOC emissions decreased from 49,790 tons in 2005 to 30,620 tons in 2013 (HKEPD, 2013). Nevertheless, the VOC species included in the emission inventory were not the same as those in this study. On the other hand, both observed and simulated O_3 increased, with a rate of 0.23 ± 0.03 and 0.16 ± 0.05 ppbv/year, respectively. The insignificant rate difference ($p > 0.05$) might be due to the inherent uncertainty in O_3 simulations caused by the
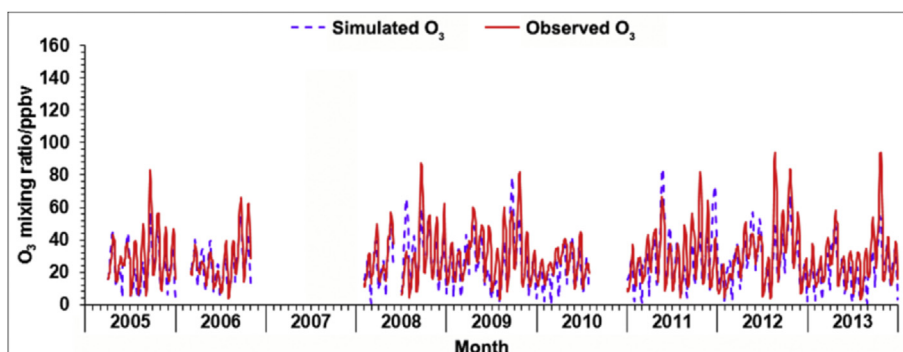

Fig. 1. Monthly average diurnal patterns of the simulated and observed O_3 between 2005 and 2013. The missing data were due to instrument maintenance.

Table 1
Hourly averages, national standards and yearly changes of main air pollutants at TC from 2005 to 2013.

Species	Hourly mean ± S.D. (ppbv)	Hourly maximum (ppbv)	National standard level II 1-hour objective (ppbv)	Yearly change rate (ppbv/year)
SO_2	5.9 ± 6.1	115.0	191	−0.44 ± 0.01
CO	636.3 ± 292.6	3204.7	8737	−17.1 ± 0.4
NO	22.6 ± 29.3	410.8	N.A.	−0.37 ± 0.04
NO_2	26.0 ± 18.7	951.8	106	−0.13 ± 0.03
NMHCs	14.7 ± 15.1	126.0	N.A.	0.34 ± 0.02
O_3	19.4 ± 19.1	184.9	106	0.23 ± 0.03
Simulated O_3	21.8 ± 19.7	174.9	106	0.16 ± 0.05

N.A.: not available.

measurement uncertainties of O_3 precursors and the possible insufficiencies of chemical mechanisms in the model. Overall, the O_3 increment indicated the increasing severity of photochemical pollution in Hong Kong. All the variations mentioned above were significant ($p < 0.05$).

3.2. Evaluation of the solvent and DCV programs

3.2.1. Tracers of solvent usage and diesel exhaust

In view of the increasing trends of total NMHCs and O_3 in these years, the effectiveness of the solvent and DCV programs, which were aimed at mitigating O_3 pollution, was evaluated. Prior to the evaluation, the VOCs tracers of solvent usage and diesel exhaust were determined. Fig. 2 shows the source profiles of VOCs emitted from solvent usage and the exhausts of diesel, LPG and gasoline fueled vehicles. These profiles were acquired from the real source emission measurements in previous studies in Hong Kong (Guo et al., 2011, 2015; Ho et al., 2009). Noticeably, toluene, ethylbenzene and xylene isomers (TEX) were the dominant VOC species in the emissions of solvent usage with a proportion (% by weight) much higher than those in other sources. Therefore, TEX were treated as the tracers of solvent usage. Diesel exhaust was distinguished by high emissions of C_2–C_4 hydrocarbons, particularly ethane, ethene and ethyne. Toluene was the most abundant aromatics in diesel exhaust, however it was much lower than that emitted from solvent usage ($p < 0.05$). Furthermore, a high percentage of ethane was also found in the exhausts of LPG and gasoline vehicles. Thus, it is not appropriate to use it as the tracer of
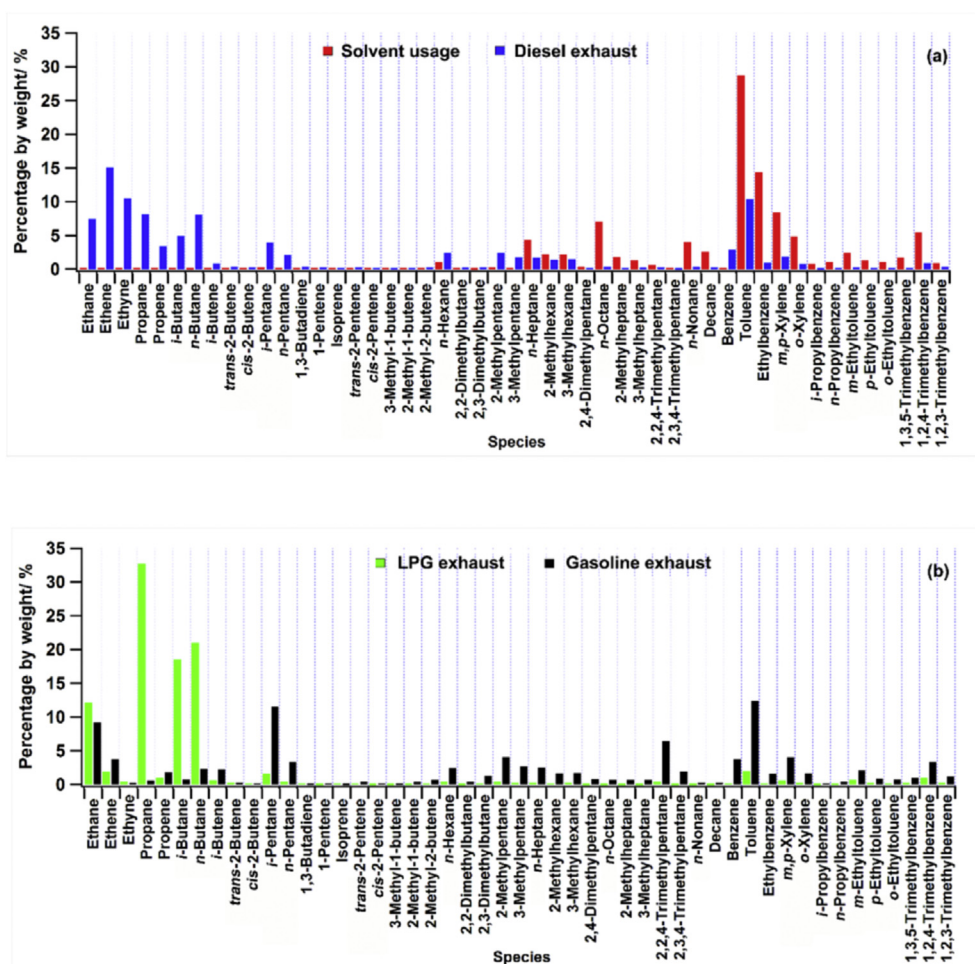

Fig. 2. (a) Source profiles of VOCs emitted from solvent usage and exhausts of diesel vehicles. (b) Source profiles of VOCs emitted from the exhausts of LPG and gasoline vehicles.

diesel vehicular exhaust. Instead, propene was a perfect tracer of diesel exhaust given its low proportion (~1% by weight) in LPG and gasoline vehicular exhausts. Because ethyne was not measured, ethene and propene were used to distinguish diesel vehicular exhaust in this study. For LPG exhaust emission, propane and i-/n-butanes were the most significant components, while i-/n-pentanes were the markers of gasoline exhaust. It should be noted that the LPG and gasoline exhausts also made some contributions to the tracers of solvent usage and diesel exhaust, which might slightly bias the evaluation of the programs when the measured concentrations of these tracers were directly used.

3.2.2. Long-term trends and monthly averages of the tracers

Fig. 3 presents the time-dependent variations of the sum of solvent usage tracers (TEX) and diesel exhaust tracers (ethene and propene) at different stages of the programs. The sum of solvent usage tracers decreased significantly during the periods of both "before-during" (2005–2011) and "during-after" (2007–2013) the solvent program, with rates of -25.6 ± 11.5 pptv/year ($0.05 < p < 0.1$) and -135.9 ± 13.9 pptv/year ($p < 0.05$), respectively. Overall, a decreasing trend was observed for the sum of solvent usage tracers from 2005 to 2013 (-99.1 ± 6.9 pptv/year, $p < 0.05$), implying the effectiveness of the solvent program on the reduction of VOCs emissions from solvent products. In contrast, the sum of diesel exhaust tracers increased significantly at 48.2 ± 2.0 pptv/year, from before to during (2005–2013) the DCV program ($p < 0.05$).

As the meteorological conditions were relatively similar in the same months of different years (Lyu et al., 2016), the comparisons of monthly averages among different stages of the programs could minimize the meteorological influences on the evaluation, as shown in Fig. S5 in the Supplementary Material. Consistent with their time-dependent variations, the sum of solvent usage tracers was generally lower "during" than "before" the solvent program ($p < 0.05$), and continued decreasing after the program, except for the insignificant changes ($p > 0.05$) in several months, i.e., May, August and October. However, the sum of diesel exhaust tracers was higher "during" the DCV program than "before" ($p < 0.05$) in most months, except for April. Again, these results indicate the success of the solvent program, but possible ineffectiveness of the DCV program. Nevertheless, we should bear in mind that both the tracers of solvent usage and diesel exhaust had other sources (e.g., LPG and gasoline exhaust). For example, LPG and gasoline vehicles also emitted large amount of ethane (see Fig. 2(b)). Hence, the source apportionment of VOCs, including the species used as the tracers, would help to more accurately evaluate the effectiveness of the programs (see section 3.2.3).

3.2.3. Source apportionment

Fig. 4 shows the source apportionment results extracted from PMF, which best reproduced the observed concentrations of VOCs and coincided with the VOCs source profiles in Hong Kong. Factor 1 had high concentrations of toluene, ethylbenzene and xylene isomers, fairly similar to the source profile of solvent usage. Therefore, this factor was assigned as solvent usage. Factor 2 was treated as diesel exhaust, in view of the relatively high concentrations of ethane, ethene and propene. However, the concentration of ethene was much lower than that of ethane in this factor, contradictory to the source profile of diesel exhaust in Fig. 2 where ethene dominated over ethane. A reasonable explanation was that ethene experienced more photochemical consumption than ethane from the emission source to the monitoring site, due to its higher
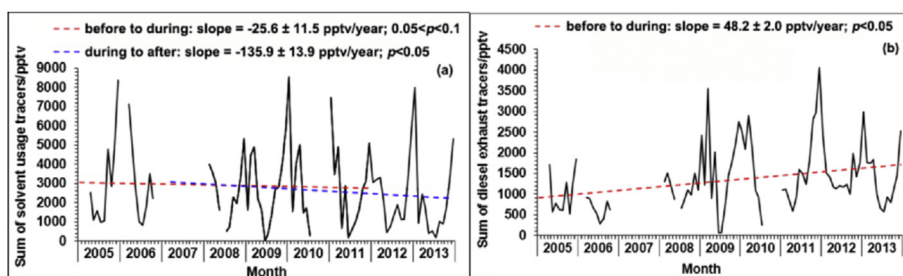

Fig. 3. Variations of the sum of solvent usage tracers and diesel exhaust tracers at different stages of (a) the solvent program and (b) the DCV program.
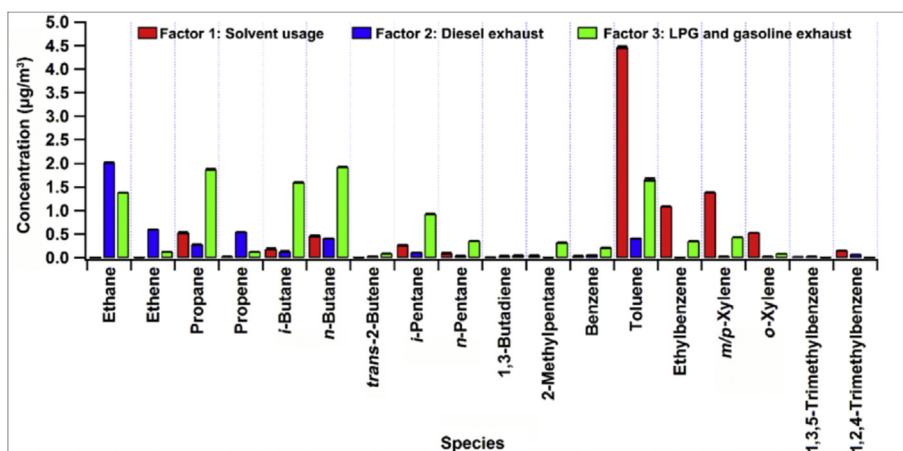

Fig. 4. Source profiles of VOCs extracted from PMF. The standard errors were estimated with the bootstrap method in PMF.

photochemical reactivity. To validate this hypothesis, the VOCs monitored at a roadside site during December 2013–May 2014 were applied to PMF for source apportionment, aiming at minimizing the influence of photochemical reactivity. The PMF-extracted source profiles were very similar to the real source profiles (see Fig. S6 in the Supplementary Material), for example, ethene in diesel exhaust was comparable to ethane, suggesting that photochemical loss was the main cause of lower ethene in diesel exhaust extracted by the PMF at TC. The last factor was likely associated with LPG and gasoline exhaust, in view of the dominance of C_3–C_5 hydrocarbons. Typically, propane and i-/n-butanes are the main species in LPG exhaust, and gasoline exhaust is characterized by high concentrations of i-/n-pentanes.

Table S3 in the Supplementary Material shows the average mass and percentage contributions of each source to the total VOCs. The gasoline and LPG vehicle emissions were the most predominant contributor to VOCs, followed by solvent usage and diesel exhaust, with mass contributions of 11.9 ± 0.1, 9.3 ± 0.1 and 4.46 ± 0.04 μg/m^3, respectively. Fig. 5 shows the long-term trends of each individual source emission extracted from the PMF. The VOCs emitted from solvent usage decreased during the study period ($p < 0.05$), with a rate of -204.7 ± 39.7 pptv/year, confirming the effectiveness of the solvent program on VOC control. The diesel exhaust related VOCs also experienced a significant decrease of -304.5 ± 17.7 pptv/year ($p < 0.01$). However, the VOCs originated from gasoline and LPG vehicle emissions noticeably increased ($p < 0.01$), with a rate of 1086 ± 34 pptv/year. The reduction of VOCs emitted from diesel exhaust obtained from PMF simulation here was inconsistent with the increase of the sum of diesel exhaust tracers (ethene and propene) in section 3.2.2. Indeed, the increase of ethene and propene was mainly attributable to the LPG and gasoline exhaust according

to the source apportionment, in which the sum of ethene and propene increased from 202.3 ± 36.3 pptv in 2005 to 676.6 ± 49.2 pptv in 2013, at an average rate of 83.2 ± 2.7 pptv/year. This rate was significantly higher than the actual increasing rate of the sum of diesel tracers (48.2 ± 2.0 pptv/year) ($p < 0.05$), indicating that the DCV program actually relieved the increasing trend of these species. The increased VOC emissions from gasoline and LPG vehicles are in line with the fact that the gasoline and LPG fueled vehicles increased from 375,641 in 2005 to 486,355 in 2013 (HKCSD, 2005, 2013). Although some measures were implemented to control the gasoline and LPG vehicle emissions (see http://www.epd.gov.hk/epd/english/environmentinhk/air/prob_solutions/air_problems.html), they were neither mandatory (e.g., tax incentives for environment-friendly petrol private cars) nor in force for a long period (e.g., the replacement of converters on LPG fueled vehicles initiated in September 2013; strengthened emission control for petrol and LPG vehicles from September 2014). As a consequence, the VOCs emitted from gasoline and LPG vehicles remarkably increased from 2005 to 2013.

3.2.4. Impact on ozone production

Given the effects of the solvent and DCV programs on VOC control, their impacts on local O_3 production were investigated using the subtraction method. Briefly, we simulated an O_3 base case using the observed VOC levels, and subtracted this from constrained cases using the VOCs in specified sources to yield the O_3 produced by VOCs in those sources. Table S4 in the Supplementary Material lists the yearly average O_3 produced by VOCs in different sources. Overall, solvent usage (1.15 ± 0.07 ppbv) and gasoline and LPG vehicle emissions (1.17 ± 0.07 ppbv) made comparable contributions to O_3 production from 2005 to 2013. O_3 produced by
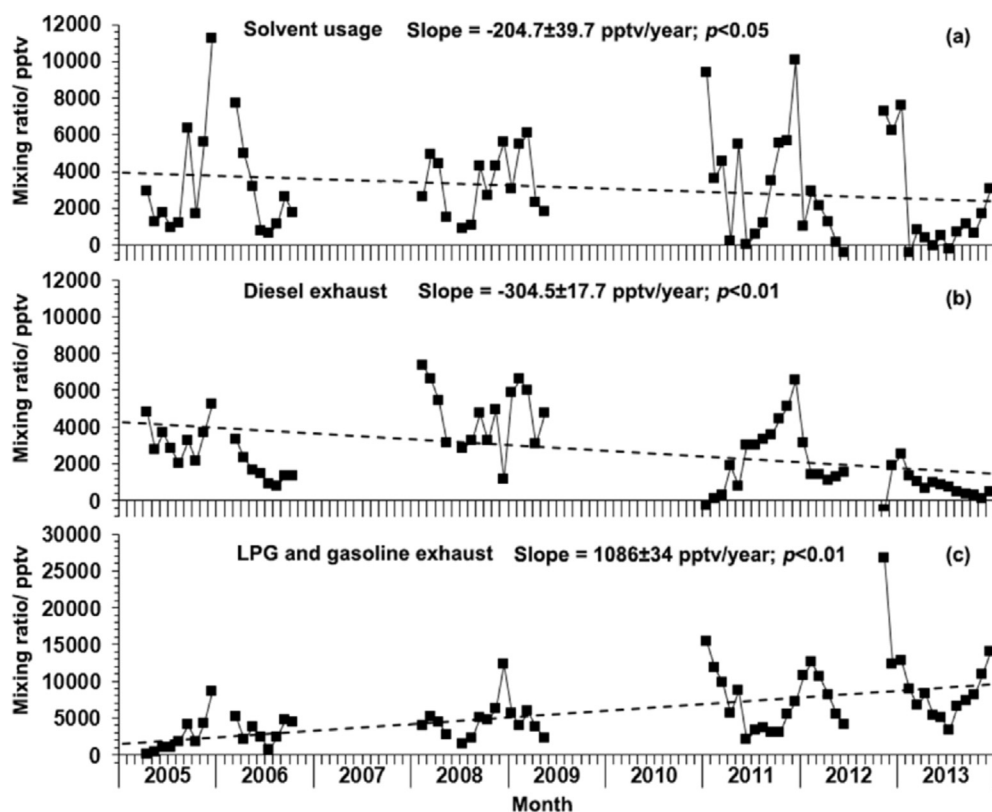

Fig. 5. Monthly variations of total VOCs originated from different sources. The ticks on the horizontal axis represent months, and the missing months were due to the filtration of local air and exclusion of missing data in each species for model input.

VOCs in diesel exhaust averaged 0.60 ± 0.03 ppbv. From 2005 to 2013, O_3 produced by solvent usage and diesel exhaust significantly decreased ($p < 0.01$), at rates of -0.16 ± 0.01 and -0.05 ± 0.01 ppbv/year, respectively. However, the VOCs emitted from gasoline and LPG vehicles made an increasing contribution to O_3 production (average rate $= 0.09 \pm 0.01$ ppbv/year) ($p < 0.01$). The source-specific O_3 variation trends coincided with the long-term trends of VOCs originating from the corresponding sources.

Table 2 summarizes the yearly O_3 changes under different actual and theoretical scenarios from 2005 to 2013. The "present" scenario (actual scenario) illustrates the O_3 changes simulated with full ambient concentrations of VOCs and NO_x, in which the effects of both solvent and DCV programs are included. The "NO_x unchanged" scenario (theoretical scenario) assumes that NO and NO_2 were unchanged between 2005 and 2013. The "original" scenario (theoretical scenario) means that the solvent and DCV programs were not implemented, specifically that O_3 produced was a result of solvent usage and diesel exhaust each year was the same as that in 2005. Finally, the "original + xx" scenarios (theoretical scenarios) reflect O_3 variations when only one of the programs (solvent or DCV program) was implemented. Overall, O_3 was predicted to increase significantly ($p < 0.05$) with an average rate of 0.39 ± 0.03 ppbv/year from 2005 to 2013 without the implementation of the DCV and solvent programs. This increment is likely to be related to the weakening of NO titration because of the observed reduction of NO (i.e., rate of -0.37 ppbv/year) in these years. In addition, O_3 produced by gasoline and LPG vehicle emissions increases by 0.09 ppbv/year. The implementation of the DCV and solvent programs significantly lessened the average increase of O_3 to 0.34 ± 0.02 and 0.23 ± 0.03 ppbv/year, respectively ($p < 0.05$). The combined effects of these two programs (the "present" scenario) still led to an O_3 increase of 0.16 ± 0.05 ppbv/year. As previously discussed, NO_x reduction is a possible reason for the O_3 increment. On the other hand, in the scenario when NO_x remained unchanged from 2005 to 2013, the O_3 increasing rate slightly decreased to 0.13 ± 0.05 ppbv/year, however the reduction was not significant ($p > 0.05$). Therefore, we conclude that the present O_3 increment was mainly due to the emission enhancement of VOCs from gasoline and LPG fueled vehicles. In addition, other sources not considered in this study might also make some contributions to O_3 increment, e.g., isoprene increased by 4.7 ± 0.2 pptv/year during the study period.

3.3. Implication for future control strategies

To improve air quality in Hong Kong, a set of emission reduction targets were endorsed by Hong Kong and Guangdong province in 2012, which regulated the reduction of VOCs and NO_x by 15% and 20−30%, respectively, by 2020 in Hong Kong using 2010 as the base year. Based on these targets, assuming that VOCs were cut by 15%, O_3 in 2020 was simulated under three scenarios with NO_x cut by 20%, 25% and 30%, respectively. The simulation results indicated that O_3 would increase by 2.4 ± 0.2, 3.1 ± 0.5 and 5.1 ± 0.5 ppbv in 2020 relative to 2010 (22.5 ± 1.5 ppbv), indicating that the O_3

increment caused by the weakening of NO titration effect was higher than the O_3 reduction through VOC control. For example, the 25% reduction of NO_x led to a simulated O_3 increment of 5.6 ± 0.5 ppbv, whereas the O_3 decrease due to 15% VOC reduction was only -2.5 ± 0.4 ppbv, giving the net O_3 increment of 3.1 ppbv. As such, more stringent VOC control measures should be formulated and implemented to prevent O_3 increases by 2020.

Based on the measured VOCs and NO_x in 2010, the net O_3 increment in 2020 relative to O_3 in 2010 was simulated with the cut of VOCs and NO_x (cut percentage of 0−50% in the interval of 10%), as shown in Fig. 6. It can be seen that the net O_3 increment increases non-linearly with the increase of NO_x cut percentage, and decreases with the increase of VOCs cut percentage, representing the VOC-limited regime in O_3 formation. Furthermore, the net O_3 increment was more sensitive to VOCs cut when NO_x was low (indicated by the line spacing), and was more sensitive to NO_x when VOCs were high (indicated by the line slopes). For example, the net O_3 increment increased by 2.8 ppbv/10% VOCs cut and 1.3 ppbv/10% VOCs cut when NO_x was cut by 50% (relatively low NO_x region) and 30% (relatively high NO_x region), respectively. However, when VOCs were cut by 30% (relatively high VOC region) and 50% (relatively low VOC region), the 50% cut of NO_x caused the O_3 increment of 10.3 and 5.3 ppbv, respectively. This was mainly because O_3 formation was favored by low NO_x and high VOCs. Moreover, to maintain nil O_3 increment, the minimum cut percentages of VOCs were approximately 30% and 50% when NO_x was cut by 20% and 30%, respectively. In other words, the reduction ratio of VOCs/NO_x should be higher than ~1.5.

4. Conclusions

During the past decade, the Hong Kong government implemented a series of control strategies to improve the air quality, including two programs aimed at emission reductions from solvent usage and diesel vehicles. Based on real-time measurements of air pollutants, the air quality in Hong Kong generally improved from 2005 to 2013. However, the photochemical pollution became more severe, characterized by an increase of O_3. The VOCs emitted from both solvent usage and diesel exhaust decreased significantly from 2005 to 2013, while VOCs emitted from gasoline and LPG vehicles showed an increasing trend. In terms of the impacts on O_3 production, both the solvent and DCV programs lessened the O_3 rate of increase, whereas O_3 was enhanced by the gasoline and LPG vehicle emissions. Lastly, model simulations indicated that O_3 would

Table 2
Average yearly increasing rates of O_3 in different scenarios from 2005 to 2013. Year 2007 was excluded due to missing data.

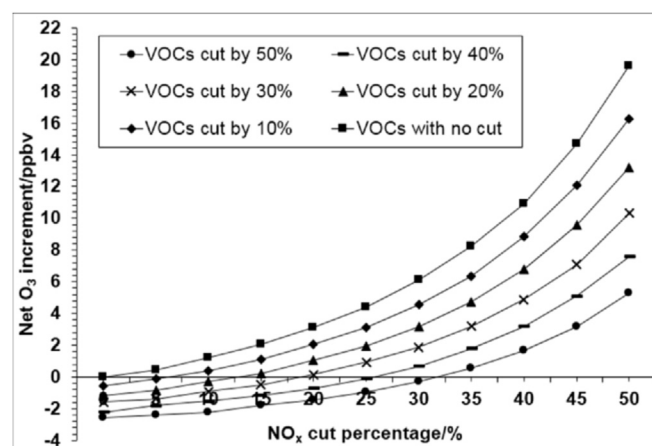| Scenarios	Yearly variation rate of O_3 (ppbv/year)
Original	0.39 ± 0.03
Original + DCV program	0.34 ± 0.02
Original + solvent program	0.23 ± 0.03
Present	0.16 ± 0.05
NO_x unchanged	0.13 ± 0.05

Fig. 6. Net O_3 increment by 2020 with the cut of VOCs and NO_x, using 2010 as the base year.

increase under the existing government-planned reduction scheme, because of increased O_3 when NO_x levels decrease, despite decreased O_3 when VOC levels decrease. Therefore to control O_3 by 2020, the reduction ratio of VOCs/NO_x should be higher than ~1.5 when NO_x is cut by 20%–30%. This study provides scientific evidence for the formulation and implementation of future air pollution control strategies in Hong Kong, which can be extended to other cities.

Acknowledgements

Appendix A. Supplementary data

Supplementary data related to this article can be found at http://dx.doi.org/10.1016/j.envpol.2016.09.025.

References

Carvalho, V.S.B., Freitas, E.D., Martins, L.D., et al., 2015. Air quality status and trends over the Metropolitan area of Sao Paulo, Brazil as a result of emission control policies. Environ. Sci. Policy 47, 68–79.

Cheng, H.R., Guo, H., Wang, X.M., et al., 2010. On the relationship between ozone and its precursors in the Pearl River Delta: application of an observation-based model (OBM). Environ. Sci. Pollut. Res. 17, 547–560.

Cheng, H.R., Saunders, S.M., Guo, H., et al., 2013. Photochemical trajectory modeling of ozone concentrations in Hong Kong. Environ. Pollut. 180, 101–110.

Cheung, K., Guo, H., Wang, X.M., et al., 2010. Diurnal profiles of isoprene, methacrolein and methyl vinyl ketone at an urban site in Hong Kong. Atmos. Environ. 84, 323–331.

Derwent, R.G., Witham, C.S., Utembe, S.R., et al., 2010. Ozone in Central England: the impact of 20 years of precursor emission controls in Europe. Environ. Sci. Policy 13, 195–204.

Ding, A.J., Wang, T., Fu, C.B., 2013. Transport characteristics and origins of carbon monoxide and ozone in Hong Kong, South China. J. Geophys. Res. Atmos. 118, 9475–9488.

Guo, H., Cheng, H.R., Ling, Z.H., et al., 2015. Report for HKEPD: Integrated Data Analysis and Characterization of Photochemical Ozone in Hong Kong. Hong Kong Environmental Protection Department, Hong Kong.

Guo, H., Jiang, F., Cheng, H.R., et al., 2009. Concurrent observations of air pollutants at two sites in the Pearl River Delta and the implication of regional transport. Atmos. Chem. Phys. 9, 7343–7360.

Guo, H., Ling, Z.H., Cheung, K., et al., 2013. Characterization of photochemical pollution at different elevations in mountainous areas in Hong Kong. Atmos. Chem. Phys. 13, 3881–3898.

Guo, H., Zou, S.C., Tsai, W.Y., et al., 2011. Emission characteristics of nonmethane hydrocarbons from private cars and taxis at different driving speeds in Hong Kong. Atmos. Environ. 45, 2711–2721.

HKCSD, 2005. Hong Kong Annual Digest of Statistics 2005 accessible at. http://www.statistics.gov.hk/pub/B10100032005AN05B0600.pdf.

HKCSD, 2013. Hong Kong Annual Digest of Statistics 2013 accessible at. http://www.statistics.gov.hk/pub/B10100032013AN13B0100.pdf.

HKEPD, 2014. Air Quality in Hong Kong 2014 accessible at. http://www.aqhi.gov.hk/en/download/air-quality-reportse469.html?showall=&start=1.

HKEPD, 2013. 2013 Hong Kong Emission Inventory Report accessible at. http://www.epd.gov.hk/epd/sites/default/files/epd/2013EIReport_eng_1b.pdf.

Ho, K.F., Lee, S.C., Ho, W.K., 2009. Vehicular emission of volatile organic compounds (VOCs) from a tunnel study in Hong Kong. Atmos. Chem. Phys. 9, 7491–7504.

Hurley, P.J., Blockley, A., Rayner, K., 2001. Verification of a prognostic meteorological and air pollution model for year-long predictions in the Kwinana industrial region of Western Australia. Atmos. Environ. 35, 1871–1880.

Lam, S.H.M., Saunders, S.M., Guo, H., et al., 2013. Modelling VOC source impacts on high ozone episode days observed at a mountain summit in Hong Kong under the influence of mountain-valley breezes. Atmos. Environ. 81, 166–176.

Lau, A.K.H., Yuan, Z., Yu, J.Z., et al., 2010. Source apportionment of ambient volatile organic compounds in Hong Kong. Sci. Total Environ. 408, 4138–4149.

Ling, Z.H., Guo, H., Lam, S.H.M., 2014. Atmospheric photochemical reactivity and ozone production at two sites in Hong Kong: Application of a Master Chemical Mechanism–photochemical box model. J. Geophys. Res. Atmos. 119, 10567–10582.

Ling, Z.H., Guo, H., 2014. Contribution of VOC sources to photochemical ozone formation and its control policy implication in Hong Kong. Environ. Sci. Policy 38, 180–191.

Ling, Z.H., Guo, H., Zheng, J.Y., et al., 2013. Establishing a conceptual model for photochemical ozone pollution in subtropical Hong Kong. Atmos. Environ. 76, 208–220.

Lippmann, M., 1992. Health effects of tropospheric ozone: review of recent research findings and their implications to ambient air quality standards. J. Expo. Anal. Environ. Epid 3, 103–129.

Lyu, X.P., Guo, H., Simpson, I.J., et al., 2016. Effectiveness of replacing catalytic converters in LPG-fueled vehicles in Hong Kong. Atmos. Chem. Phys. 16, 6609–6626.

Ou, J.M., Guo, H., Zheng, J.Y., et al., 2015. Concentrations and sources of non-methane hydrocarbons (NMHCs) from 2005 to 2013 in Hong Kong: a multi-year real-time data analysis. Atmos. Environ. 103, 196–206.

Paatero, P., 1997. Least squares formulation of robust non-negative factor analysis. Chemom. Intell. Lab. 37, 23–35.

Paatero, P., Tapper, U., 1994. Positive matrix factorization: a non-negative factor model with optimal utilization of error estimates of data values. Environmetrics 5, 111–126.

Scheff, P.A., Wadden, R.A., 1993. Receptor modeling of volatile organic compounds. 1. Emission inventory and validation. Environ. Sci. Technol. 27, 617–625.

Thurston, G.D., Ito, K., 1999. Epidemiological studies of ozone exposure effects. Air Pollut. Health 1, 485–509.

Xue, L.K., Wang, T., Louie, P.K.K., et al., 2014. Increasing external effects negate local efforts to control ozone air pollution: a case study of Hong Kong and implications for other Chinese cities. Environ. Sci. Technol. 48, 10769–10775.

Zhang, J., Wang, T., Chameides, W.L., et al., 2007. Ozone production and hydrocarbon reactivity in Hong Kong, Southern China. Atmos. Chem. Phys. 7, 557–573.